Nature of the quantum metal in a two-dimensional crystalline superconductor

Evidence for a Bose Metal in a Two-Dimensional Crystalline Superconductor

A. W. Tsen[1], B. Hunt[1†], Y. D. Kim[2], Z. J. Yuan[3], S. Jia[3,4], R. J. Cava[5], J. Hone[2], P. Kim[6], C. R. Dean[1*] and A. N. Pasupathy[1*]

[1]Department of Physics, Columbia University, New York, NY 10027, USA

[2]Department of Mechanical Engineering, Columbia University, New York, NY 10027, USA.

[3]International Center for Quantum Materials, Peking University, Beijing 100871, China.

[4]Collaborative Innovation Center of Quantum Matter, Beijing 100871, China

[5]Department of Chemistry, Princeton University, Princeton, NJ 08544, USA.

[6]Department of Physics, Harvard University, Cambridge, MA 02138, USA.

[†]Current address: Department of Physics, Carnegie Mellon University, Pittsburgh, PA 15213, USA.

*Correspondence to: cd2478@columbia.edu, apn2108@columbia.edu

Two-dimensional (2D) materials are not expected to be metals at low temperature due to electron localization[1]. Consistent with this, pioneering studies on thin films reported only superconducting and insulating ground states, with a direct transition between the two as a function of disorder or magnetic field[2-5]. However, more recent work has revealed the presence of an intermediate metallic state occupying a substantial region of the phase diagram[6-9], whose nature is intensely debated[10-16]. Here, we observe such a state in the disorder-free limit of a crystalline 2D superconductor, produced by mechanical co-lamination of $NbSe_2$ in inert atmosphere. Under a small perpendicular magnetic field, we induce a transition from a superconductor to the intermediate metallic state. We find a new power law scaling with field in this phase, which is consistent with the Bose metal model where metallic behavior arises from strong phase fluctuations caused by the magnetic field[10-13].

Global superconductivity emerges in a sample when conduction electrons form Cooper pairs and condense into a macroscopic, phase-coherent quantum state. In two dimensions, the phase coherence can be disrupted even at zero temperature by increasing disorder—either by degrading sample quality or by applying magnetic fields to create vortices[1]. Granular or amorphous superconducting thin films, for which disorder levels can be varied during growth, have thus provided an established platform for the study of quantum phase transitions in 2D superconductors. Within the conventional theoretical framework, increasing sample disorder or magnetic field perpendicular to a strongly disordered film at $T = 0$ induces a direct transition to an insulating state as the normal state sheet resistance approaches the pair quantum resistance $h/(2e)^2 = 6.4\text{k}\Omega$[1,3]. As film quality improved over time, however, an intervening metallic phase with resistance much lower than the normal state resistance has been observed in several systems with generally less disorder[6-9]. Its origin is not well understood, and the various theoretical treatments can be divided between bosonic-based models, in which Cooper pairing persists in the metallic phase but phase coherence is lost[10-13], and models that also incorporate other fermionic degrees of freedom[14-16].

Recently, mechanical exfoliation has emerged as a technique to produce ultra-clean, crystalline 2D materials, with graphene being a well-known example[17]. Like amorphous films, the thickness of these samples can be easily controlled down to the level of individual atomic layers. In contrast to amorphous films, a 2D superconductor exfoliated from a layered, single crystal, can exist in the regime of minimal disorder, allowing for new insight into the nature of the vortex state in two dimensions. In this work, we realize such a system using a clean bilayer of $NbSe_2$, a well-known, type-II superconductor with $T_c \sim 7.2\text{K}$ in bulk form[18,19]. Unique to this sample, the normal state sheet resistance is two orders of magnitude below $h/(2e)^2$ and insulating

behavior is never observed. Instead, the intermediate metallic phase emerges in an exceptionally large region of the magnetic field-temperature phase diagram. Unlike the typical exponential behavior associated with the quantum tunneling of fermionic quasiparticles[6,14], we observe a new power law scaling as a function of field at low temperature that is consistent with the Bose metal scenario of the metallic phase[10-13].

Initial studies on exfoliated $NbSe_2$ flakes do not observe a superconducting transition to a zero-resistance state in the atomically thin limit[20,21]. Recently, however, it has been shown the surfaces of metallic materials may oxidize, altering the electronic properties of thin samples[22]. Exfoliation and encapsulation by a protective layer in inert atmosphere is thus crucial for preserving the intrinsic properties of the 2D material[22,23]. We achieve this using a mechanical transfer setup installed inside a nitrogen-filled glove box (see Methods). In short, within the glove box, an exfoliated $NbSe_2$ flake is electrically contacted by graphite (G), and the entire device is protected by an insulating layer of hexagonal boron nitride (BN). The graphite leads are then contacted using an edge-metallization technique in the ambient environment[24,25]. A schematic depicting the assembly and fabrication process is shown in Figure 1a and optical images of the heterostructure are shown in Figure 1b before (left) and after device fabrication.

In the main panel of Figure 2a, we show four-terminal sheet resistance as a function of temperature for a particular $NbSe_2$ device prepared using the method described above. The $NbSe_2$ thickness is 1.5nm as determined by an atomic force microscope (AFM), suggesting it consists of only two atomic layers. The resistance in the normal state is R_N = 75Ω. This corresponds to a residual resistivity that is 10 times larger than that of bulk crystals[19], yet the sheet resistance is still an order of magnitude less than that of the most conductive amorphous superconducting films[9]. We observe a clear superconducting transition to a zero-resistance state

measured to the limit of our instrument resolution. The critical temperature is T_c = 5.26K, as defined by where the resistance is 90% of the normal state value, which is slightly reduced from the transition temperature of bulk samples (7.2K)[18,19].

In order to further characterize the quality and dimensionality of our sample, we measured the temperature-dependent critical fields, defined by $R(H_{c2}, T) = 0.9R_N$, for field configuration both perpendicular and parallel to the layers, and the results are plotted in the inset of Figure 2a. Close to T_c, we expect $H_{c2}^{\perp} = \frac{\phi_0}{2\pi\xi_0^2}\left(1 - \frac{T}{T_c}\right)$, where ϕ_0 is the flux quantum and ξ_0 is the in-plane coherence length at zero temperature[26]. A linear fit shown by the black line yields ξ_0= 8.9nm, similar to the bulk value[18,19]. From the normal state residual resistance and carrier concentration as determined by Hall measurements, we estimate the electron mean free path to be l = 17nm, smaller than that in bulk crystals[19], but nearly twice the coherence length, confirming that our device is in the pure superconductor regime[26]. In contrast, amorphous films are generally characterized as "dirty" superconductors with $\xi_0 \ll l$. The critical parallel field does not exhibit linear temperature dependence expected for anisotropic 3D superconductors[26]. Instead, a 2D superconductor with thickness $d < \xi_0$ obeys $H_{c2}^{\parallel} = \frac{\sqrt{12}\phi_0}{2\pi\xi_0 d}\sqrt{1 - \frac{T}{T_c}}$[27]. The red curve in the inset of Figure 2a shows a best fit to this expression, from which we extract d = 3.4nm, which is slightly larger than the thickness as determined by AFM (1.5nm). However, this fitting has been previously found to overestimate the true sample thickness in sufficiently thin systems[27].

The superconducting phase transition in a 2D material with $d < \xi_0$ is understood to be of the Berezinskii-Kosterlitz-Thouless (BKT) type[28]. In this scenario, the low-temperature, zero-resistance phase consists of bound vortex-antivortex pairs created by thermal fluctuations. Upon

heating, the pairs dissociate and may move, inducing dissipation. The BKT temperature defines the vortex unbinding transition and can be determined using current-voltage measurements as a function of temperature T, as shown in the main panel of Figure 2b. Current excites free-moving vortices, causing a nonlinear voltage dependence: $V \sim I^{a(T)}$. At T_{BKT}, a 2D superconductor obeys the universal scaling relation, $V \sim I^3$ (solid line in Fig. 2b)[28,29]. In the inset, we plot a vs. T, as determined by the slope of the different V-I traces in log-log scale. An example guide-to-eye fit is marked by the dashed line in the main panel. We determine T_{BKT} = 5.01 K from where a = 3 interpolates, only slightly less than T_c as defined above. This is consistent with the behavior of systems with normal state resistance much less than $h/(2e)^2$, where T_{BKT} is expected to be very close to the mean-field transition temperature[30].

The measurements performed above confirm that our device exhibits the characteristics of a true 2D superconductor. The extracted material parameters together with the low normal state sheet resistance further places the high sample quality within a previously unexplored regime. We next turn to the dependence of resistance on perpendicular magnetic field as the effect of vortices can now be cleanly separated from the low static disorder present in the sample. Shown in Figure 3a is a 2D color map of the four-terminal sheet resistance in the same device as a function of both temperature and magnetic field applied perpendicular to the layers. For clarity, temperature traces for different field levels are shown in an Arrhenius plot in Figure 3b. For fields larger than $H_{c2} \sim$ 3T, the sample is in the normal state for all temperatures. Previous works on strongly disordered films observed a field-tuned transition to an insulating state[4,5]; however, one might not expect insulating behavior for finite samples of a highly conductive 2D system in the disorder-free limit[9]. We have applied perpendicular fields as large

as 14.5T and still see metallic behavior with dR/dT > 0 in the temperature dependence (see Supplementary Information, Figure S1 main panel).

As one lowers the field to just below H_{c2}, a resistance drop is observed upon cooling from the normal state. In this region of the H-T phase diagram, the device exhibits activated behavior, as can been seen in the linear slope in the Arrhenius plot (black lines in Fig. 3b). Classically, dissipation in a superconductor in which resistance is less than the normal state value can be attributed to the motion of individual vortices (flux creep or flow)[26]. In a clean 2D system, we expect the dominant energy barrier to flux motion to be that of vortex-antivortex dissociation[31]. Flux resistance then becomes thermally activated when the temperature is comparable to the barrier energy. We have determined the activation energy from linear portion of the Arrhenius plot in Figure 3b for different magnetic fields, and the result is plotted in Figure 3c. The functional form is expected to be $U(H) = U_0 \ln(H_0/H)$, where $U_0 \sim \frac{{\phi_0}^2 d}{256\pi^3\lambda^2}$, the vortex-antivortex binding energy, and $H_0 \sim H_{c2}$[6,31]. A fit to this form yields U_0 = 27.5K and H_0 = 2T for our device. Assuming the magnetic penetration depth λ is similar to the bulk value (230nm)[18], we estimate $U_0 \sim$ 14K, on the order of the experimental value.

At lower temperatures, the resistance saturates to a level dependent on magnetic field (see colored lines in Fig. 3b), hallmark of the anomalous metallic state that is the main subject of this report. Qualitatively similar behavior has also been observed in amorphous MoGe and Ta films with much larger normal state sheet resistances[6,8]. This effect cannot be understood within a classical framework, in which we expect to recover superconductivity for $T \ll U$. In the past, various theories have been advanced to explain the origin of dissipation in this temperature regime for disordered films[10-16]. One can distinguish between the different models based on the magnetic field dependence of the saturated resistance at low temperatures.

Shimshoni et al. consider a disordered superconducting film as a percolating network of superconducting islands within an insulating matrix[14]. Field-induced vortices that tunnel across thin superconducting constrictions give rise to resistance when coupled to a fermionic bath. The resistance depends on field as $R = \frac{h}{4e^2} exp\left[C\frac{\pi}{2}\left(\frac{\hbar/e^2}{R_N}\right)\left(\frac{H-H_{c2}}{H_{c2}}\right)\right]$, where R_N is the normal state resistance and C is a dimensionless constant of order unity. This expression finds good agreement with the measurements of Ephron *et al.* on amorphous MoGe films, in which $R_N \sim$ 1kΩ(*6*), but evidently provides a poor fit to our data (see Supplementary Information, Figure S2). Furthermore, since our device is over an order of magnitude more conductive, the closest fitting requires $C = 0.14$, an unphysically small value.

Galitski et al. consider a "vortex metal" phase where field-induced vortices interact with electrically neutral spinons[16]. The theory accounts for the large peak in low-temperature magnetoresistance observed in disordered InOx films before saturation to R_N at higher fields[9]. In our device, however, we observe a monotonic dependence of resistance on field and see no peak structure in magnetoresistance up to 7T (see Supplementary Information, Figure S1 inset).

Das and Doniach, as well as Dalidovich and Phillips, report that a 2D system of interacting bosons may form a gapless, nonsuperfluid state in the limit of zero temperature, a phase which they term a "Bose metal"[10-13]. They argue that the uncondensed Cooper pairs and vortices are responsible for the small resistance observed at small finite field[11]. A magnetic field introduces gauge fluctuations, which disrupts phase coherence and causes dissipation, a quantum analog of that caused by thermal fluctuations in the BKT transition. In the Bose metal model, resistance on the metallic side of the field-tuned transition can be described by: $R \sim (H - H_{c0})^{2\nu}$, where H_{c0} is the critical field of the superconductor to Bose metal transition and ν is the

exponent of the superfluid correlation length, which diverges across the boundary as $(H - H_{c0})^{-\nu}$[11].

In the main panel of Figure 4a, we show a log-log plot of R vs $H - H_{c0}$ taken at several different temperatures. H_{c0} is a small temperature dependent value which we determined using a method that shall be described below. The linear scaling observed here suggests a power law dependence on field. We have fit the data to the expression $R \sim (H - H_{c0})^{\square}$ and the extracted exponent $\mapsto$ is plotted in the inset as a function of temperature. At high temperatures, but below T_c, resistance increases roughly linearly with field, as expected for unhindered flux flow: $R \sim R_N H/H_{c2}$ ($\mapsto = 1$)[26]. The gray line shows linear scaling as a guide-to-eye. As temperature is lowered, the field dependence becomes increasingly nonlinear and collapses onto a single curve below 1K with $\mapsto \sim 3$. The red line is an empirical fit given by $R = 5.44\left[\frac{\Omega}{T^3}\right](H - 0.15T)^{3.21}$, which shows excellent agreement with the data. This yields a critical exponent of $\nu = 1.61$. While previous measurements on both MoGe and InOx films at the lowest accessible temperatures observe mostly an exponential dependence of resistance with field, which is consistent with quantum tunneling of fermionized vortices[9,32], at small very fields for the MoGe film, however, the scaling obeys a power law with unity exponent[32]. The power law scaling we observe in our sample consistently over the entire field range thus suggests that the fermionic behavior undergoes a crossover to that of a Bose metal in the limit of ultra-low disorder.

The critical field of the transition out of the true zero-resistance state H_{c0} is difficult to determine directly from the linear resistance given the limited accuracy of our instruments. Recently, however, experiments by Qin *et al.* and Li *et al.* on disordered Ta films showed that H_{c0} can be determined indirectly using current-voltage measurements[8,33]. Hysteresis is observed in the *V-I* characteristics on the superconducting side, similar to that seen in underdamped

Josephson junctions[26], which disappear at the onset of the metallic phase. We have performed *V*-*I* measurements on the same device at T = 0.5K for increasing magnetic fields (see Supplementary Information, Figure S3 main panel). Clear hysteresis is seen between current sweep up and down for low fields. In the inset, we plot the current hysteresis δI for where the voltage jump occurs as a function of magnetic field. δI vanishes close to H_{c0} = 0.175T. This then allows us to identify the true superconducting phase as that for $H < H_{c0}$. We have repeated this measurement for several different temperatures in order to determine critical field as a function of temperature.

Figure 4b shows a full *H*-*T* phase diagram for our device. The blue triangles mark $H_{c0}(T)$ and the red circles mark $H_{c2}^{\perp}(T)$. The boundary between Bose metal and flux flow (purple squares) is defined by the intersection of the fits to the activated resistance and saturated levels in Figure 3b. The normal phase extends up to at least 14.5T without the appearance of an insulating phase, in contrast to previous works on strongly disordered films. The high sample quality is made possible by our facile device assembly technique in inert atmosphere, which demonstrates a new route for the production of 2D superconductors in the ultraclean limit.

Methods

Crystal Synthesis

Polycrystalline $NbSe_2$ was made by heating stoichiometric amount of Nb powder (99.5%) and Se shots (99.999%) in evacuated silica ampules. Single crystals of $NbSe_2$ were grown using a vapor transfer method. 400 mg of $NbSe_2$ powder and 80 mg of I_2 were sealed in a 23cm long silica ampule with a 1.13 cm^2 inner cross section. The charge was put in the hot zone of 850℃ and the sink in the cold zone of 750℃. After one week, all the polycrystals became single crystals, with most of the thicker plates found in the hot zone.

Device Assembly and Fabrication

We have exfoliated ultrathin $NbSe_2$ flakes in a nitrogen-filled glove box containing less than 2ppm oxygen. Separately, we prepared thin hexagonal boron nitride (BN) on a polydimethylsiloxane (PDMS) stamp covered with polypropylene carbonate (PPC), which we use to "pick up" two closely spaced graphite flakes (separation ~ 2μm). The BN/graphite stack is then used to cover the $NbSe_2$ flake inside the glove box. While graphite makes electrical contact to $NbSe_2$, hBN provides an insulating oxidation barrier. Subsequent lithography may then be used to define a four-terminal device, in which the gapped region between the graphite leads form the channel. The graphite is then electrically contacted using an edge-metallization technique[24,25].

References

1. Goldman, A. M. & Markovic, N. Superconductor-insulator transitions in the two-dimensional limit. *Physics Today* **51**, 39-44 (1998).
2. Haviland, D. B., Liu, Y., & Goldman, A. M. Onset of superconductivity in the two-dimensional limit. *Physical Review Letters* **62**, 2180-2183 (1989).
3. Fisher, M. P. A. Quantum phase transitions in disordered two-dimensional superconductors. *Physical Review Letters* **65**, 923-926 (1990).
4. Hebard, A. F. & Paalanen M. A. Magnetic-field-tuned superconductor-insulator transition in two-dimensional films. *Physical Review Letters* **65**, 927-930 (1990).
5. Yazdani, A. & Kapitulnik, A. Superconducting-insulating transition in two-dimensional ↦-MoGe thin films. *Physical Review Letters* **74**, 3037-3040 (1995).

6. Ephron, D., Yazdani, A., Kapitulnik, A., & Beasley, M. R. Observation of quantum dissipation in the vortex state of a highly disordered superconducting thin film. *Physical Review Letters* **76**, 1529-1532 (1996).

7. Christiansen, C., Hernandez, L. M., & Goldman, A. M. Evidence of collective charge behavior in the insulating state of ultrathin films of superconducting metals. *Physical Review Letters* **88**, 037004 (2002).

8. Qin, Y. G., Vicente, C. L., Yoon, J. Magnetically induced metallic phase in superconducting tantalum films. *Physical Review B* **73**, 100505 (2006).

9. Steiner, M. A., Breznay, N. P., & Kapitulnik, A. Approach to a superconductor-to-Bose-insulator transition in disordered films. *Physical Review B* **77**, 212501 (2008).

10. Das, D. & Doniach, S. Existence of a Bose metal at T=0. *Physical Review B* **60**, 1261-1275 (1999).

11. Das, D. & Doniach, S. Bose metal: gauge-field fluctuations and scaling for field-tuned quantum phase transitions. *Physical Review B* **64**, 134511 (2001).

12. Dalidovich, D. & Phillips, P. Phase glass is a Bose metal: A new conducting state in two dimensions. *Physical Review Letters* **89**, 027001 (2002).

13. Phillips, P. & Dalidovich, D. The elusive Bose metal. *Science* **302**, 243-247 (2003).

14. Shimshoni, E., Auerbach, A. & Kapitulnik, A. Transport through quantum melts. *Physical Review Letters* **80**, 3352-3355 (1998).

15. Spivak, B., Zyuzin, A., Hruska, M. Quantum superconductor-metal transition. *Physical Review B* **64**, 132502 (2001).

16. Galitski, V. M., Refael, G., Fisher, M. P. A. & Senthil, T. Vortices and quasiparticles near the superconductor-insulator transition in thin films. *Physical Review Letters* **95**, 077002 (2005).

17. Geim, A. K. & Novoselov, K. S. The rise of graphene. *Nature Materials* **6**, 183-191 (2007).

18. de Trey, P., Gygax, S. & Jan, J.-P. Anisotropy of the Ginzburg-Landau parameter in $NbSe_2$. *Journal of Low Temperature Physics* **11**, 421 (1973).

19. Soto, F. *et al.*, Electric and magnetic characterization of $NbSe_2$ single crystals: anisotropic superconducting fluctuations above T_c. *Physica C-Superconductivity and Its Applications* **460**, 789-790 (2007).

20. Staley, N. E. *et al.*, Electric field effect on superconductivity in atomically thin flakes of $NbSe_2$. *Physical Review B* **80**, 184505 (2009).

21. El-Bana *et al.*, M. S. Superconductivity in two-dimensional $NbSe_2$ field effect transistors. *Superconductor Science & Technology* **26**, 125020 (2013).

22. Tsen, A. W. *et al.* Structure and control of charge density waves in two-dimensional 1T-TaS_2, arXiv:1505.03769 [condmat] (2015)

23. Cao, Y. *et al.* Quality heterostructures from two-dimensional crystals unstable in air by their assembly in inert atmosphere. *Nano Letters ASAP* (2015).

24. Wang, L. *et al.*, One-dimensional electrical contact to a two-dimensional material. *Science* **342**, 614-617 (2013).

25. Cui, X. *et al.*, Multi-terminal transport measurements of MoS_2 using a van der Waals heterostructure device platform. *Nature Nanotechnology* **10**, 534-540 (2015).

26. Tinkham, M. *Introduction to Superconductivity* 2nd edn (Dover, 1996).

27. Kim, M., Kozuka, Y., Bell, C., Hikita, Y., & Hwang, H. Y. Intrinsic spin-orbit coupling in superconducting δ-doped $SrTiO_3$ heterostructures. *Physical Review B* **86**, 085121 (2012).

28. Halperin, B. I. & Nelson, D. R. Resistive transition in superconducting films. *Journal of Low Temperature Physics* **36**, 599-616 (1979).

29. Eley, S., Gopalakrishnan, S., Goldbart, P. M., Mason, N. Approaching zero-temperature metallic states in mesoscopic superconductor-normal-superconductor arrays. *Nature Physics* **8**, 59-62 (2012).

30. Beasley, M. R., Mooij, J. E., & Orlando, T. P. Possibility of vortex-antivortex pair dissociation in two-dimensional superconductors. *Physical Review Letters* **42**, 1165-1168 (1979).

31. Feigelman, M. V., Geshkenbein, V. B., & Larkin, A. I. Pinning and creep in layered superconductors. *Physica C* **167**, 177-187 (1990).

32. Mason, N. & Kapitulnik, A. True superconductivity in a two-dimensional superconducting-insulating system. *Physical Review B* **64**, 060504 (2001).

33. Li, Y., Vicente, C. L., & Yoon, J. Transport phase diagram for superconducting thin films of tantalum with homogeneous disorder. *Physical Review B* **81**, 020505 (2010).

Acknowledgements

We acknowledge helpful discussions with Z. Han, J.-D. Pillet, E. Shimsoni, O. Vafek, A. Kapitulnik, D. Xiao, and D. Gopalan. This material is based upon work supported by the NSF MRSEC program through Columbia in the Center for Precision Assembly of Superstratic and Superatomic Solids (DMR-1420634). Salary support is provided by the NSF under grants NEB-1124894 (A.W.T.) and DMR-1056527 (A.N.P.). Some measurements were performed at the

National High Magnetic Field Laboratory, which is supported by the NSF Cooperative Agreement (DMR-0654118), the State of Florida and the Department of Energy. S.J. is supported by the National Basic Research Program of China (grants 2013CB921901 and 2014CB239302). R.J.C. is supported by the Department of Energy, Division of Basic Energy Sciences (grant DOE FG02-98ER45706). P.K. acknowledges support from the Army Research Office (grant W911NF-14-1-0638).

Author contributions:

A.W.T, B.H., C.D., and A.N.P. conceived and designed the experiment. Z.J.Y., S.J., and R.J.C. synthesized the $NbSe_2$ crystals. A.W.T. fabricated the devices with assistance from Y.D.K.. A.W.T. and B.H. performed the transport measurements. A.W.T, B.H., C.D., and A.N.P. analyzed the data and wrote the paper.

Competing financial interests:

The authors declare no competing financial interests.

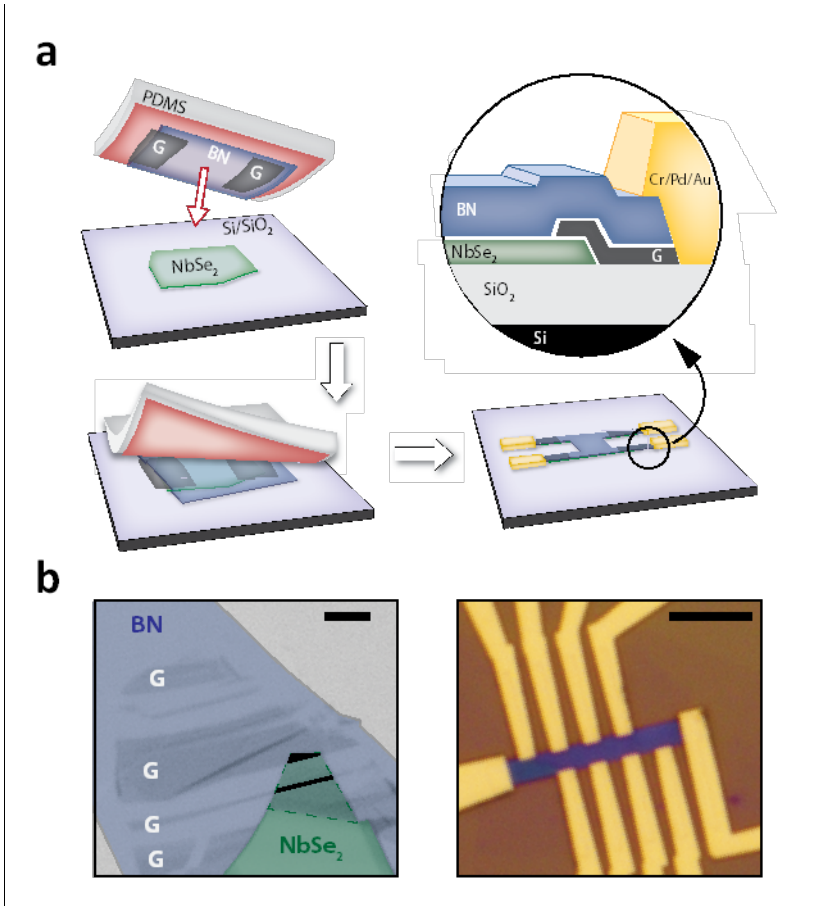

Figure 1 | Environmentally controlled device fabrication. a. Schematic of heterostructure assembly process. Boron nitride (BN)/graphite (G) on a polymer stamp (PDMS) is used to electrically contact and encapsulate $NbSe_2$ in inert atmosphere. The heterostructure is lithographically patterned and the edge of graphite is metalized with Cr/Pd/Au. **b.** Optical images of heterostructure before (left) and after device fabrication (right). In the (false-colored) left panel, the bilayer $NbSe_2$ is outlined in a dashed green line and the overlap between the graphite and bilayer $NbSe_2$ is shaded black. Scale bar is 5μm in both images.

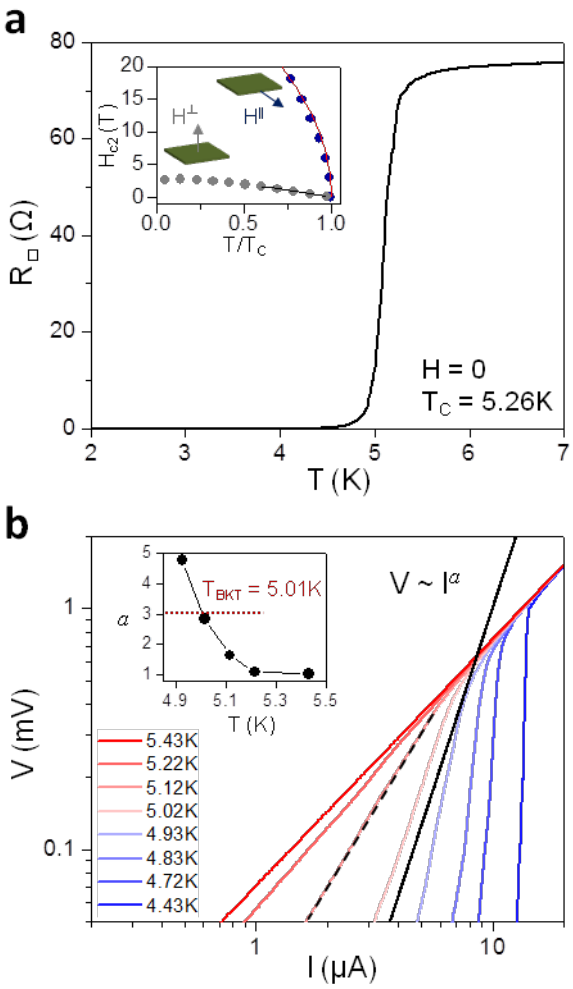

Figure 2 | Characterization of bilayer $NbSe_2$ device. a. Sheet resistance with temperature shows superconducting transition at T_c = 5.26K. Temperature-dependent critical magnetic fields parallel and perpendicular to the layers are shown in the inset. Black line is linear fit to $H_{c2}^{\perp} \propto 1 - T/T_c$ at high temperatures. Red line is fit to $H_{c2}^{\parallel} \propto \sqrt{1 - T/T_c}$, the Tinkham formula for 2D samples(*26*). **b.** Voltage-current behavior at different temperatures. Inset shows exponent a vs. T extracted from power law fitting $V \sim I^a$ near the normal state transition. a = 3 at the BKT temperature 5.01K.

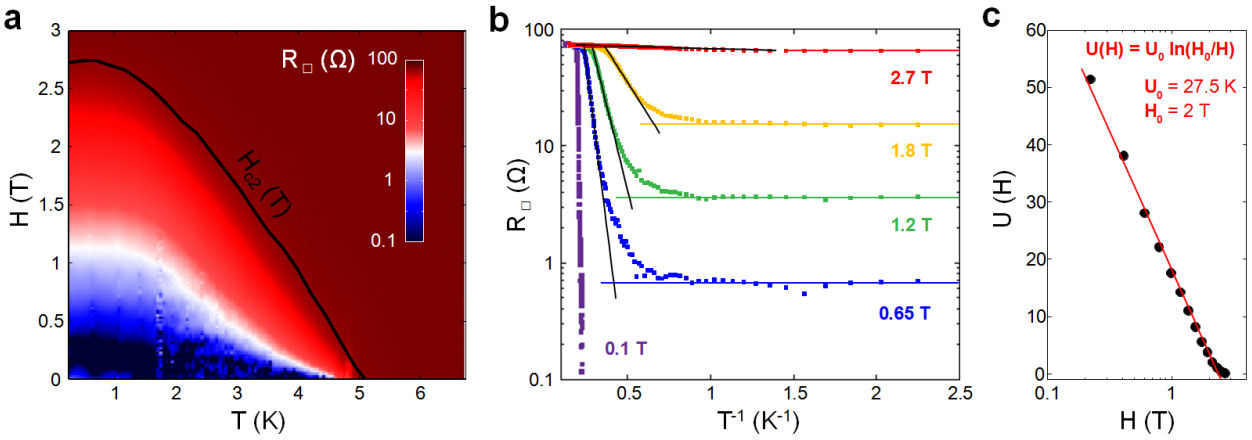

Figure 3 | Magnetic field tuned phase transitions in 2D $NbSe_2$. a. 2D color plot of sheet resistance vs. temperature and perpendicular magnetic field. The black line marks $H_{c2}(T)$. **b.** Arrhenius plot of resistance for several magnetic fields shows thermally activated regime (black lines) and saturation at low temperatures (colored lines). **c.** Energy barrier vs. magnetic field extracted from linear fit to activated region. Solid red line is empirical fit to formula in inset.

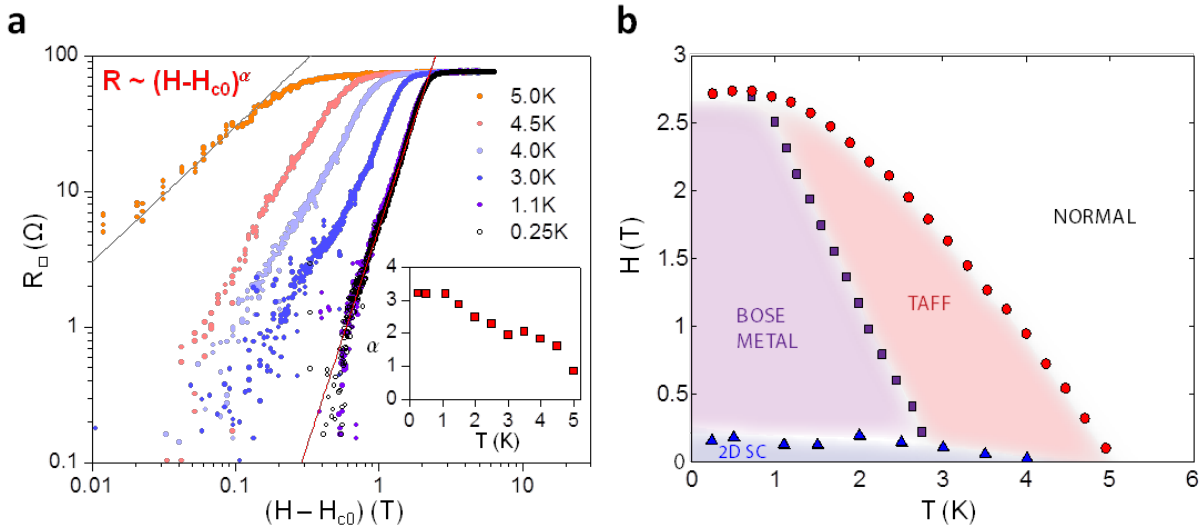

Figure 4 | Emergence of the Bose metal. a. Magnetoresistance below the superconducting transition for different temperatures. The data scale to a power law $R \sim (H - H_{c0})^{\mapsto(T)}$ and collapse onto a single curve in the Bose metal phase below 1K. $\mapsto$ vs. T is plotted in inset. Gray line guide-to-eye linear scaling (high T) and red line is empirical fit to Bose metal scaling (low T). **b.** Full H-T phase diagram of bilayer $NbSe_2$ device. The red circles are $H_{c2}(T)$. The purple squares, dividing the Bose metal from the thermally assisted flux flow (TAFF) regime, mark the transition from activated behavior $R \sim \exp(U(H)/T)$ to temperature-independent resistance $R = R(H)$, i.e. the intersection of the black and colored lines in Fig. 3b. The blue triangles denote the boundary of the superconducting phase $H_{c0}(T)$. This criterion is determined by when hysteresis vanishes in V-I measurements (see Fig. S3).

SUPPLEMENTARY INFORMATION

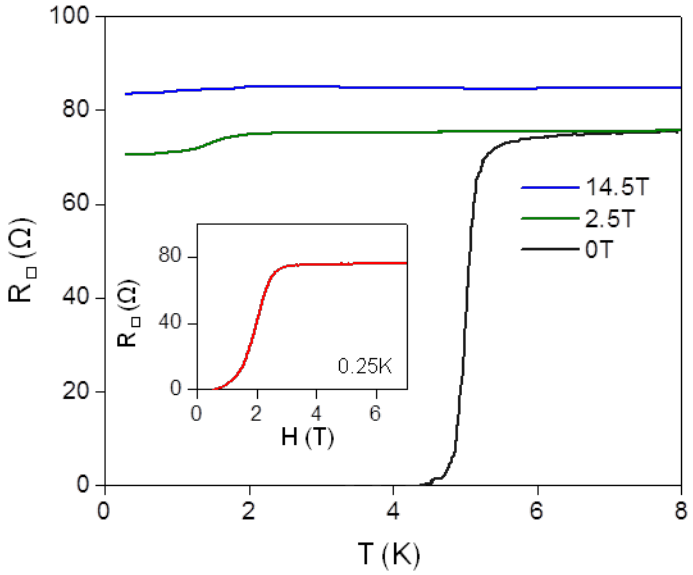

Figure S1 | Behavior at higher magnetic fields. Sheet resistance with temperature for several different perpendicular fields. No insulating behavior is observed up to 14.5T. Inset shows magnetoresistance at 0.25K. No peak is observed up to 7T.

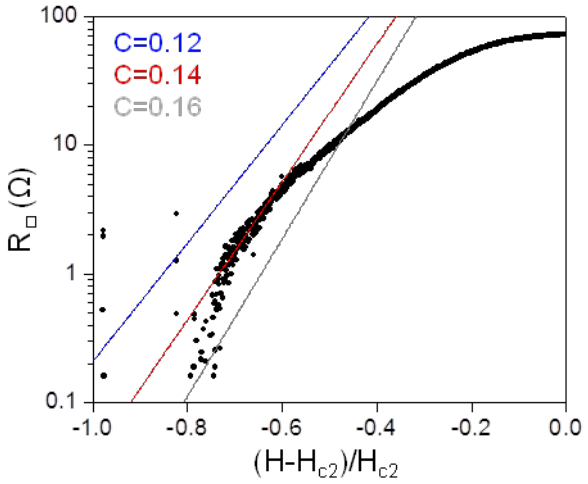

Figure S2 | **Vortex tunneling scenario.** Magnetoresistance at 0.25K fit to the formula in Shimshoni *et al.* describing quantum tunneling of vortices with several different values for constant C[14]. Best fitting ($C = 0.14$) deviates significantly at higher fields.

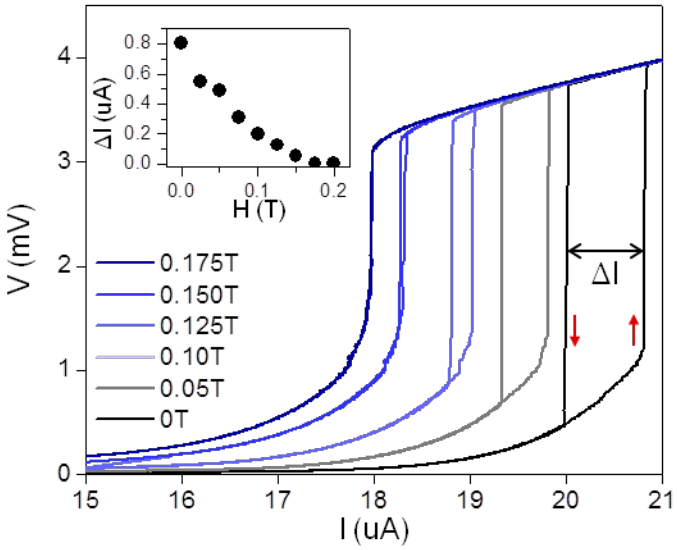

Figure S3 | Field-tuned voltage-current characteristics. *V-I* traces at 0.5K for several perpendicular field levels. Inset shows hysteresis between current sweep up and sweep down as a function of field. Hysteresis is observed in the superconducting phase, $H < H_{c0} = 0.175$T, but disappears for the metallic phase, $H > H_{c0}$.